J|A|C|S
ARTICLES
Published on Web 10/19/2004

The Structure of Ba@C_{74}

Andreas Reich,[†] Martin Panthöfer,[†] Hartwig Modrow,[‡] Ulrich Wedig,[†] and Martin Jansen*,[†]

Contribution from the Max Planck Institute for Solid State Research, Heisenbergstr. 1, D-70569 Stuttgart, Germany, and Institute of Physics of the University of Bonn, Nussallee 12, D-53115 Bonn, Germany

Received July 8, 2004; E-mail: M.Jansen@fkf.mpg.de

Abstract: The title compound has been produced by using the radio frequency (RF) method. Barium and carbon were evaporated simultaneously under dynamic flow of helium at different temperatures. About 0.5 mg of pure Ba@C_{74} was isolated via a three-step high-pressure liquid chromatography separation. For the first time, the structure of a monometallofullerene has been analyzed by means of single-crystal synchrotron diffraction on microcrystals of Ba@C_{74}·Co(OEP)·2C_6H_6 (Co^{II}(OEP): cobalt(II) octaethylporphyrin) at 100 K. The monometallofullerene exhibits a high degree of localization of the endohedral metal ion, with just two split positions for Ba and two orientations of the C_{74}-cage. The barium atom is localized inside the C_{74}-cage and displaced off-center, toward the Co(OEP) molecule ($d \approx 127$ pm). The shortest Ba−C distance is 265 pm. The Co(OEP) molecules form dimers in which the coordination of the cobalt is (4 + 1). Due to the all-syn conformation of the ethyl groups, each Co(OEP) molecule of the dimer coordinates one C_{74}-fullerene. The units (Ba@C_{74})[Co(OEP)]$_2$(Ba@C_{74}) are arranged in a distorted primitive hexagonal packing. The free space between these complex units is filled by benzene molecules of crystallization. The Ba L_{III} XANES spectrum of a thin film sample of Ba@C_{74} exhibits a pronounced double maximum structure at about $E = 5275$ eV. The comparison of the shape resonances of the experimental data with simulated XANES spectra, based on different exo- and endohedral structure models, confirm that the Ba atom is located inside the C_{74}-cage (D_{3h}) in an off-center position. The Ba atom is shifted by about 130−150 pm from the geometric center of the C_{74}-cage. This is in good agreement with quantum chemical results. Thus, despite the disorder still present, a consistent and conclusive structure model for the title compound has been derived by employing a combination of X-ray diffraction, XANES spectroscopy, and quantum chemical calculations.

Introduction

Even though the production of fullerenes and endohedral fullerenes has been well-known since the discovery of this family of carbon allotropes,[1,2] there is still lack of reliable structural data. Besides the non-IPR endohedral metal fullerenes Sc_2@C_{66}[3] and Sc_3N@C_{68},[4] there is no final proof for the endohedral character of the smaller size cages monometallo fullerenes MC_n ($n < 78$). This is due to the very small amounts of these fullerenes available. In particular, no experimental structural investigations have been reported for the C_{74}-cage so far, neither for the normal nor for the endohedrally functionalized one. This is partly due to the low electronic band gap and the resulting high reactivity of the empty C_{74}-cage.[5] Upon exohedral reduction, i.e., by means of electrochemical methods, the resulting dianion, C_{74}^{2-}, is a stable closed shell molecule. Analogously, endohedral reduction by an incorporated divalent metal atom, i.e., the formation of M^{II}@C_{74}, leads to stable compounds, which have been isolated and investigated by means of spectroscopic methods.[6−9] Furthermore, mono-, di-, and trimetallo endohedral fullerenes of trivalent metals have been reported.[10−15]

A small number of single-crystal X-ray structure analyses of co-crystallizates of metal octaethylporphyrin and empty or

[†] Max Planck Institute for Solid State Research.
[‡] Institute of Physics of the University of Bonn.

(1) Kroto, H. W.; Heath, J. R.; O'Brien, S. C.; Curl, R. F.; Smalley, R. E. *Nature* **1985**, *318*, 162−163.
(2) Chai, Y.; Guo, T.; Jin, C. M.; Haufler, R. E.; Chibante, L. P. F.; Fure, J.; Wang, L. H.; Alford, J. M.; Smalley, R. E. *J. Phys. Chem.* **1991**, *95*, 7564−7568.
(3) Takata, M.; Nishibori, E.; Sakata, M.; Wang, C. R.; Shinohara, H. *Chem. Phys. Lett.* **2003**, *372*, 512−518.
(4) Olmstead, M. M.; Lee, H. M.; Duchamp, J. C.; Stevenson, S.; Marciu, D.; Dorn, H. C.; Balch, A. L. *Angew. Chem., Int. Ed.* **2003**, *42*, 900−905.
(5) Diener, M. D.; Alford, J. M. *Nature* **1998**, *393*, 668−671.
(6) Grupp, A.; Haufe, O.; Jansen, M.; Mehring, M.; Panthöfer, M.; Rahmer, J.; Reich, A.; Rieger, M.; Wie, X.-W. *AIP Conference Proceedings* **2002**, *633*, 31−34.
(7) Wan, T. S. M.; Zhang, H. W.; Nakane, T.; Xu, Z. D.; Inakuma, M.; Shinohara, H.; Kobayashi, K.; Nagase, S. *J. Am. Chem. Soc.* **1998**, *120*, 6806−6807.
(8) Haufe, O.; Reich, A.; Möschel, C.; Jansen, M. *Z. Anorg. Allg. Chem.* **2001**, *627*, 23−27.
(9) Kuran, P.; Krause, M.; Bartl, A.; Dunsch, L. *Chem. Phys. Lett.* **1998**, *292*, 580−586.
(10) Shinohara, H.; Yamaguchi, H.; Hayashi, N.; Sato, H.; Ohkohchi, M.; Ando, Y.; Saito, Y. *J. Phys. Chem.* **1993**, *97*, 4259−4261.
(11) Lian, Y. F.; Shi, Z. J.; Zhou, X. H.; He, X. R.; Gu, Z. N. *Carbon* **2000**, *38*, 2117−2121.
(12) Sueki, K.; Akiyama, K.; Yamauchi, T.; Sato, W.; Kikuchi, K.; Suzuki, S.; Katada, M.; Achiba, Y.; Nakahara, H.; Akasaka, T.; Tomura, K. **1997**, *5*, 1435−1448.
(13) Tagmatarchis, N.; Aslanis, E.; Prassides, K.; Shinohara, H. *Chem. Mater.* **2001**, *13*, 2374−2379.
(14) Okazaki, T.; Lian, Y. F.; Gu, Z. N.; Suenaga, K.; Shinohara, H. *Chem. Phys. Lett.* **2000**, *320*, 435−440.
(15) Sun, D. Y.; Liu, Z. Y.; Guo, S. H.; Xu, W. G.; Liu, S. Y. *Fullerene Sci. Technol.* **1997**, *5*, 137−147.

10.1021/ja0401693 CCC: $27.50

endohedral fullerenes, in particular those containing the so-called TNT (trimetallic nitride template) unit, have been recently carried out.[4,16−21] An overview of these structure analyses, the typical crystallographic perils encountered, and a discussion of the reliability of some of these studies can be found in ref 22.

Theoretical investigations on metallofullerenes involving the C_{74}-cage have been performed for the electronic structure of the idealized (D_{3h}) Gd and La endohedral species[23] as well as for the geometric structures of Ca@C_{74} and Sc_2@C_{74}[24] and the dynamics of Eu@C_{74}[25] and Ca@C_{74}.[26]

Experimental Section

This section consists of three parts: synthesis and crystal growth, the experimental investigation by means of single-crystal synchrotron radiation diffraction and XANES experiments, and the theoretical calculations. There is an important interplay between the second and third part, as the results from theory were necessary in order to interpret the measurements.

Preparation of Ba@C$_{74}$. Endohedral barium fullerenes were synthesized using the RF method.[27,28] Details of the experimental setup as well as the isolation by means of multistep HPLC of Ba@C_{74} are reported elsewhere.[8,29]

Crystal Growth of Ba@C$_{74}$·Co(OEP)·2C$_6$H$_6$. Crystals of Ba@C_{74}·Co(OEP)·2C_6H_6 were obtained by layering a solution of ca. 0.5 mg of Ba@C_{74} in 0.5 mL of benzene (flesh-colored) on top of a red solution of 2.5 mg of Co(OEP) in 1.5 mL of chloroform, in a glass tube. Over a period of 5 days, the two layers were allowed to interdiffuse, under reduced temperature and exclusion of light. Finally, the mother liquid was decanted, and small, dark red, rhombic crystals were harvested.

X-ray Data Collection and Structure Determination. All crystals were immersed in a light perfluoropolyether and removed from the glass tube with a small plastic loop. A crystal was mounted on a glass tip and placed in a cold nitrogen stream (100 K) on a Huber diffractometer equipped with a Bruker AXS SMART CCD 6000 detector at the beamline X3A1 at the National Synchrotron Light Source at Brookhaven National Laboratory.

Crystal data: Ba@C_{74}·Co(OEP)·2C_6H_6, formula weight = 1774.1 g mole^{-1}, monoclinic, space group $C2$ (No. 5), dark red rhombuses, 40 × 40 × 20 μm^3, a = 25.169(3) Å, b = 15.018(3) Å, c = 19.429(4) Å, β = 93.30(2)°, V = 7332(2) Å^3, Z = 4, λ = 64.3 pm, D_c = 1.6067(5) Mg m^{-3}, $2\Theta_{max}$ = 34.04°; T = 100 K, 18 394 reflections collected; 7590 independent (R_{int} = 0.132) included in the refinement; no absorption correction performed. The refinement was performed by means of full matrix least squares based on F using Jana2000,[30] 97 parameters, R_{all} = 0.265, wR_{all} = 0.186 for all data; R_o = 0.131, wR_o = 0.146, GOF(all/obsd) = 2.44/2.93. Technical details about the structure solution and refinement are published elsewhere.[22]

XANES. The sample was prepared as a thin film, by drop coating of a pure solution of Ba@C_{74} in CS_2 onto a 25 μm Kapton-foil that was glued on top of a 1 mm silica glass plate. To prevent the drop from spreading too widely, the liquid was deposited at the edge of a second, small piece of 25 μm Kapton-foil that had been glued onto the first one. After evaporation of the solvent, the thin film was sealed with a 7.5 μm Kapton-foil. All manipulations were carried out under inert gas conditions.

Ba L_{III} XANES spectra were recorded in fluorescence mode at the beamline BN2 in the ELSA synchrotron radiation laboratory in Bonn, Germany. During the measurements, the storage ring was operated at 2.3 GeV electron energy; average currents were about 50 mA. Technical details on the experimental setup are given elsewhere.[31] The energy range between 5230 and 5300 eV was scanned in steps of approximately 0.25 eV, using a set of Ge(220) crystals ($2d$ = 4.00 Å) as monochromator. Energy calibration was performed relative to a titanium reference foil, assigning a photon energy of 4966 eV to the first inflection point of the Ti K-edge spectrum. The integration time per data point was set to 2 s. Due to the limited amount of sample material available, three scans were accumulated to improve data quality. Furthermore, a linear background correction and Fourier-filtering were performed.

Quantum Chemical Calculations (QCC). Molecular density functional calculations with a LDA functional (exchange: Slater $\rho^{4/3}$, correlation: Vosko, Wilk, Nusair[32]), applying the RI-DFT formalism [33,34] as well as molecular Hartree−Fock calculations, were performed with the TURBOMOLE program package.[35] The basis set was composed of a split valence basis (SV[36]) at the carbon atoms and a 10 valence electron quasirelativistic pseudopotential[37] together with the [4s3p3d] basis supplied with TURBOMOLE for the barium atom.

The ab initio molecular dynamics calculations as well as structure optimizations with a conjugate gradient procedure were performed with the CPMD program.[38] Since CPMD uses periodic boundary conditions, the size of the cubic unit cell containing one Ba@C_{74} had to be chosen large enough to minimize intermolecular interactions. For the calculations presented, the size of the cell and the cutoff parameter, both determining the size of the plane wave basis set, were set to 18.0 Å and 45 Ry, respectively. Shrinking the cell parameter down to 14 Å or enlarging the cutoff up to 60 Ry did not change the results significantly. The quasi-relativistic pseudopotentials, with four valence electrons for C and 10 valence electrons for Ba, were taken from the work of Hartwigsen et al.[39] together with the corresponding LDA functional.[40] Various other combinations of pseudopotentials and functionals were tested for the BaC_2 molecule. These investigations are summarized in the Supporting Information.

Computational FEFF8. For the ab initio calculation of XAS spectra, the FEFF8 code was used. Detailed information on this self-consistent one-electron real-space Green's function approach is found in the

(16) Stevenson, S.; Rice, G.; Glass, T.; Harich, K.; Cromer, F.; Jordan, M. R.; Craft, J.; Hadju, E.; Bible, R.; Olmstead, M. M.; Maitra, K.; Fisher, A. J.; Balch, A. L.; Dorn, H. C. *Nature* **1999**, *401*, 55−57.
(17) Olmstead, M. M.; de Bettencourt-Dias, A.; Duchamp, J. C.; Stevenson, S.; Dorn, H. C.; Balch, A. L. *J. Am. Chem. Soc.* **2000**, *122*, 12220−12226.
(18) Olmstead, M. M.; de Bettencourt-Dias, A.; Duchamp, J. C.; Stevenson, S.; Marciu, D.; Dorn, H. C.; Balch, A. L. *Angew. Chem., Int. Ed.* **2001**, *40*, 1223−1225.
(19) Olmstead, M. M.; Lee, H. M.; Stevenson, S.; Dorn, H. C.; Balch, A. L. *Chem. Commun.* **2002**, 2688−2689.
(20) Olmstead, M. M.; de Bettencourt-Dias, A.; Stevenson, S.; Dorn, H. C.; Balch, A. L. *J. Am. Chem. Soc.* **2002**, *124*, 4172−4173.
(21) Stevenson, S.; Olmstead, M. H.; Lee, H. M.; Kozikowski, C.; Stevenson, P.; Balch, A. L. *Chem.−Eur. J.* **2002**, *8*, 4528.
(22) Friese, K.; Panthöfer, M.; Wu, G.; Jansen, M. *Acta Crystallogr., Sect. B* **2004**, *60*, 520−527.
(23) Lu, J.; Zhang, X.; Zhao, X. *Appl. Phys. A* **2000**, *70*, 461−464.
(24) Nagase, S.; Kobayashi, K.; Akasaka, T. *THEOCHEM* **1999**, *461−462*, 97−104.
(25) Vietze, K.; Seifert, G.; Fowler, P. W. *AIP Conference Proceedings* **2000**, *544*, 131−134.
(26) Shiga, K.; Ohno, K.; Kawazoe, Y.; Maruyama, Y.; Hirata, T.; Hatakeyama, R.; Sato, N. *Mater. Sci. Eng. A* **2000**, *290*, 6−10.
(27) Peters, G.; Jansen, M. *Angew. Chem., Int. Ed. Engl.* **1992**, *31*, 223−224.
(28) Jansen, M.; Peters, G.; Wagner, N. *Z. Anorg. Allg. Chem.* **1995**, *621*, 689−693.
(29) Reich, A. Synthese und Strukturaufklärung neuer endohedraler Fullerene, Ph.D. Thesis, University of Stuttgart, 2003.
(30) Petricek, V.; Dusek, M. *JANA 2000, The crystallographic computing system*; Institute of Physics, Praha: 2003.
(31) Janssen, J.; Rumpf, H.; Modrow, H.; Rablbauer, R.; Frommeyer, G.; Hormes, J. *Z. Anorg. Allg. Chem.* **2003**, *629*, 1701−1708.
(32) Vosko, S. H.; Wilk, L.; Nusair, M. *Can. J. Phys.* **1980**, *58*, 1200−1211.
(33) Eichkorn, K.; Treutler, O.; Öhm, H.; Häser, M.; Ahlrichs, R. *Chem. Phys. Lett.* **1995**, *242*, 652−660.
(34) Eichkorn, K.; Treutler, O.; Öhm, H.; Häser, M.; Ahlrichs, R. *Chem. Phys. Lett.* **1995**, *240*, 283−289.
(35) Ahlrichs, R. *TURBOMOLE*, version 5.3; Quantum Chemistry Group, Universität Karlsruhe: 2000.
(36) Schäfer, A.; Horn, H.; Ahlrichs, R. *J. Chem. Phys.* **1992**, *97*, 2571−2577.
(37) Kaupp, M.; Schleyer, P. v. R.; Stoll, H.; Preuss, H. *J. Chem. Phys.* **1991**, *94*, 1360−1366.
(38) *CPMD*, version 3.7.1; Copyright IBM Corp. 1990−2001, Copyright MPI für Festkörperforschung, Stuttgart: 1997−2001.
(39) Hartwigsen, C.; Goedecker, S.; Hutter, J. *Phys. Rev. B* **1998**, *58*, 3641−3662.
(40) Goedecker, S.; Teter, M.; Hutter, J. *Phys. Rev. B* **1996**, *54*, 1703−1710.

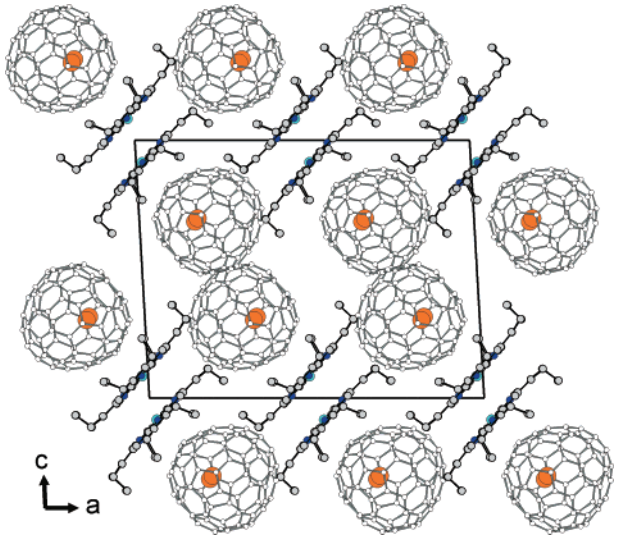

Figure 1. Unit cell of $Ba@C_{74}$·$Co(OEP)$·$2C_6H_6$ (view on plane (010), benzene molecules are not shown for clarity).

literature.[41,42] Several other studies, e.g.,[43−45] have demonstrated the successful reproduction of XANES spectra and their detailed analysis which can be achieved following this approach. Whereas the works cited so far mainly discuss systems with extended lattice symmetry, the applicability of the method to clusters had also been proven before.[46] To provide the geometrical input for the code, three structural models for two different exo-positions, referred to as exo1 and exo2, and one endo-position, all obtained from quantum chemical calculations (Figure S4), have been used.

Results

X-ray Crystal Structure Analysis. All details of the nonconventional structure solution and the special refinement strategies are reported in a more specialized publication.[22] The X-ray structure analysis unambiguously proves the endohedral character of the $Ba@C_{74}$ molecule.

The compound crystallizes in the monoclinic space group *C*2 (No. 5); the unit cell contains four crystallographically independent molecules; Co(OEP), $Ba@C_{74}$, and two benzene molecules of crystallization (Figure 1).

Each $Ba@C_{74}$ molecule is coordinated by one cobalt porphyrin complex. Due to the all-syn conformation of the OEP, the carbon cage is coordinated by the eight ethyl groups. This is in contrast to the ruffled conformation of the ethyl groups in the crystal structure of pure Co(OEP),[47] but in accordance with crystal structures of other fullerene−Co(OEP) complexes.[4,16−21] The solvent molecules, benzene, coordinate neither to OEP nor to the fullerene.

Figure 2 shows a subunit of the crystal structure. One can clearly see the concave surface formed by the all-syn conformation of the ethyl groups. This conformation allows the formation

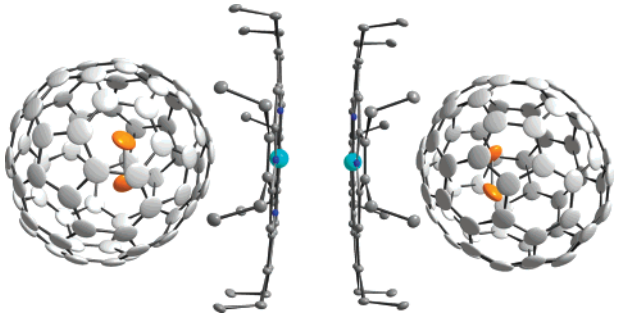

Figure 2. $(Ba@C_{74})[Co(OEP)]_2(Ba@C_{74})$ unit in $Ba@C_{74}$·$Co(OEP)$·$2C_6H_6$ (only one fullerene orientation given for clarity).

of back-to-back Co(OEP) dimers. Within these dimers, the individual OEP molecules are shifted against each other, resulting in a coordination number of 4 + 1 for Co in these dimers (Figure S1). The in-plane Co−N distances vary between 192 and 210 pm; the apical Co(1)−N′ distance is 305 pm. The angle N−Co···Co′ between the porphyrin plane and the apical N′ atom is 61.1°, and perpendicular to this direction approximately 90°.

Each Co(OEP) molecule within the dimers coordinates one $Ba@C_{74}$ molecule, resulting in complex units $(Ba@C_{74})[Co(OEP)]_2(Ba@C_{74})$ (Figure 2). The overall crystal structure of $Ba@C_{74}$·$Co(OEP)$·$2C_6H_6$ may be regarded as a distorted, primitive hexagonal packing of the dimer units. The empty space between these complex units is filled with benzene molecules of crystallization.

Two crystallographically different Ba positions, with occupancies of 0.63 and 0.37, are found inside the fullerene. The spatial separation between these two positions is 166 pm. Both Ba atom positions are shifted off the geometric center (black circles, Figure S1) of the C_{74}-cage toward the Co(OEP) complex. The displacement of the Ba positions from the geometric center is about 127 pm.

The structure exhibits an orientational disorder of the C_{74}-cage (Figure S1), with virtually equal occupancies (0.54 and 0.46). Thus, four different schemes of Ba-to-fullerene coordination have to be considered. Parts a and c in Figure 3 display a comparison of the first coordination sphere for both Ba positions and orientation A of the cage, while parts b and d give the same for the orientation B of the C_{74}-molecule. The central 6:6 bond and C atoms of the pyracylene units, which are localized on the horizontal mirror plane of the ideal C_{74}-cage (see QCC), are marked in black.

XANES. The experimental XANES spectrum of an amorphous thin film sample of $Ba@C_{74}$ exhibits a well-pronounced double maximum structure at 5271 and 5279 keV in the shape resonance area (Figure 4). It was compared to simulated XANES spectra obtained at different levels, i.e., different treatment of the core hole present in the XAS experiment (see Discussion), for two exohedral, and a set of different endohedral configurations. The double maximum structure is exclusively reproduced in the case of (i) the endohedral configuration and (ii) a displacement of the endohedral atom from the center of gravity of the C_{74} cage toward the central 6:6 bond of one of the three pyracylene units at the horizontal mirror plane by 130 to 150 pm (see Discussion).

Quantum Chemical Calculations (QCC). In agreement with earlier experimental and theoretical work,[5] we confirm C_{74} and

(41) Modrow, H.; Bucher, S.; Rehr, J. J.; Ankudinov, A. L. *Phys. Rev. B* **2003**, *67*.
(42) Ankudinov, A. L.; Ravel, B.; Rehr, J. J.; Conradson, S. D. *Phys. Rev. B* **1998**, *58*, 7565−7576.
(43) Modrow, H.; Bucher, S.; Hormes, J.; Brinkmann, R.; Bonnemann, H. *J. Phys. Chem. B* **2003**, *107*, 3684−3689.
(44) Hallmeier, K. H.; Uhlig, I.; Szargan, R. *J. Electron Spectrosc. Relat. Phenom.* **2002**, *122*, 91−96.
(45) Chen, L. X.; Liu, T.; Thurnauer, M. C.; Csencsits, R.; Rajh, T. *J. Phys. Chem. B* **2002**, *106*, 8539−8546.
(46) Ankudinov, A. L.; Rehr, J. J.; Low, J. J.; Bare, S. R. *Top. Catal.* **2002**, *18*, 3−7.
(47) Scheidt, W. R.; Turowskatyrk, I. *Inorg. Chem.* **1994**, *33*, 1314−1318.

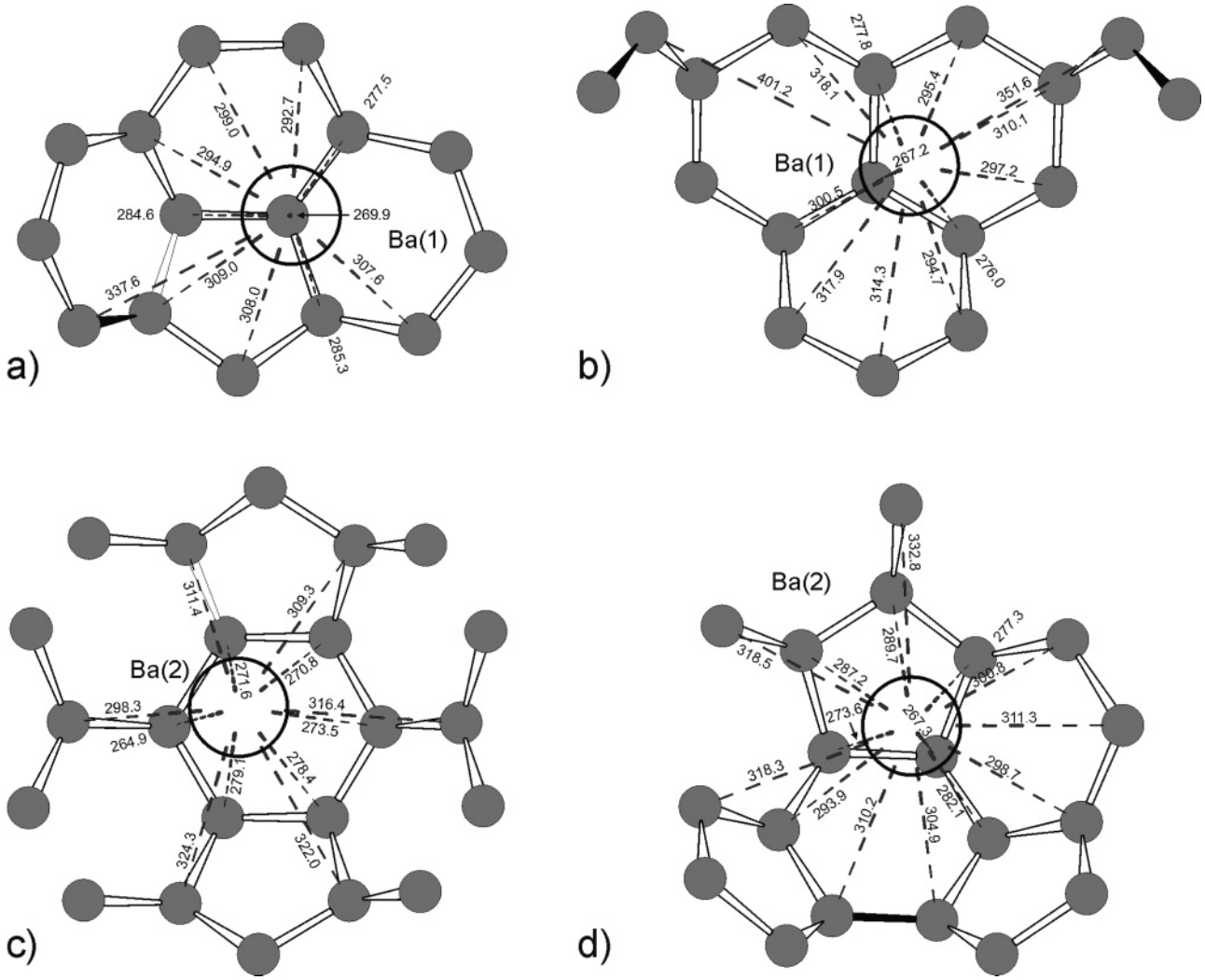

Figure 3. Coordination schemes corresponding to the different orientations of the fullerene cage and the split positions of the endohedral Ba atom. In parts a and c, both barium positions are displayed relative to orientation A of the C_{74}-molecule, and in parts b and d, the same applies for orientation B (distances given in pm). The central 6:6 bonds of the pyracylene units shown are marked in black (see QCC).

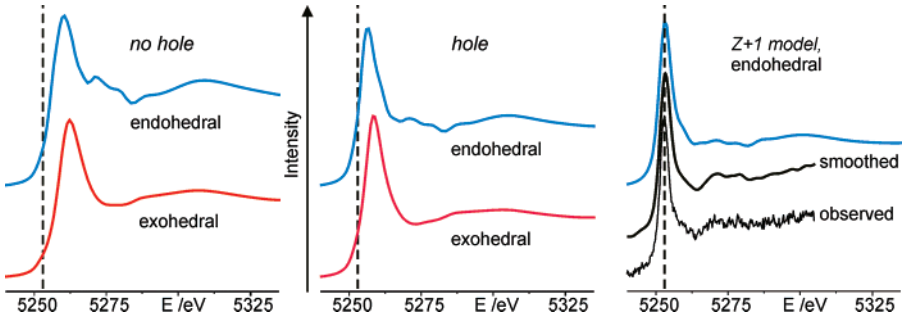

Figure 4. Calculated and measured Ba L_{III} XANES spectra of Ba@C_{74}, position of experimental white line indicated by vertical dashed lines. (Left) Calculated spectra for the exo- and endohedral case. (Middle) Calculated spectra for the exo- and endohedral cases including a core hole treatment. (Right) Experimental, smoothed and calculated spectra for the endohedral case using a $Z + 1$ model for core-hole treatment.

C_{74}^{2-} to belong to small and mid band gap species (Figure S2), with HOMO−LUMO separations of 35 and 756 meV, respectively, at the DFT-LDA level. The structural changes of C_{74} upon 2-fold reduction are found to be highly localized in the central 6:6 bond of the pyracylene units (Figure 5, emphasized by bold black lines).

Due to the additional charges, all C−C bond lengths are slightly increased by on average $\overline{\Delta d} = 0.2(9)$ *pm* (Figure S3). The particular lengthening of the central 6:6 bond of the pyracylene units ($\Delta d = 2.8$ pm) in C_{74}^{2-} reflects the antibonding contributions of the LUMO of neutral C_{74}. Compared to C_{74}^{2-}, the band gap of the endohedral Ba@C_{74} is lowered to 561 meV. The optimized structure of Ba@C_{74} corresponds to one of the 3-fold degenerate minima with the Ba atom displaced from the geometrical center of the cage in direction D (Figure 5), coordinating the central 6:6 bond of a pyracylene unit.

The calculated lengths of the shortest Ba−C distance of Ba@C_{74} depend on the method (DFT or HF) and the parameters

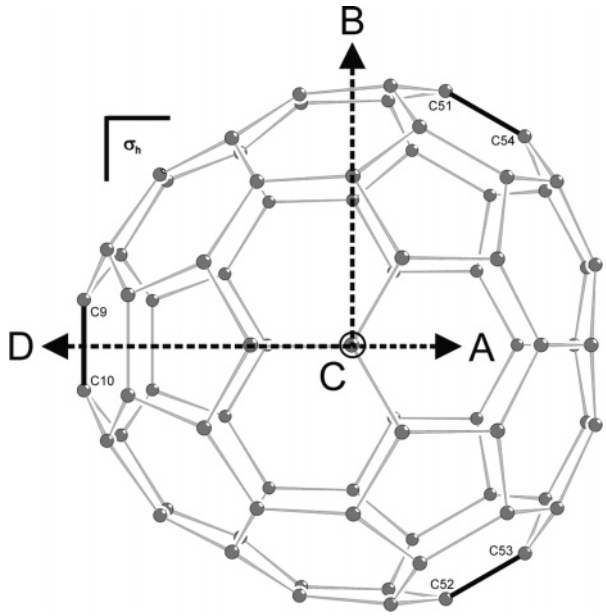

Figure 5. Calculated (RIDFT-LDA) molecular structure of C_{74}^{2-} (view along the 3-fold axis of the C_{74}^{2-}-cage). The central 6:6 bonds of the pyracylene units, which are located on the horizontal mirror plane of the C_{74}^{2-}-cage (D_{3h}), are emphasized by bold black lines. The directional vectors A, B, C, D correspond to the displacements of the endohedral Ba atom of Ba@C_{74}, as discussed in the text.

(pseudopotentials and basis sets) used. At the DFT level, the shortest distance varies between 278−289 pm. Thus, the Ba atom is moved away from the center of the cage by 135−148 pm toward one of the three symmetry-equivalent pyracylene units at the horizontal mirror plane. The results of the calculations on the HF level show a shift of the Ba atom from the center of the cage of 102 pm, which corresponds to a shortest Ba−C distance of 317 pm. On the DFT level, only slight changes of the molecular structure of the cage are observed in comparison to the dianion C_{74}^{2-}. Due to the coordination of the inner molecular surface by the Ba atom, the central 6:6 bond of the corresponding pyracylene unit is lengthened ($\Delta d = 1.9$ pm). Further variations of the C−C bond length are negligible ($\Delta d = 0.0(4)$ *pm*); i.e., the molecular structures of the carbon cage of C_{74}^{2-} and Ba@C_{74} are virtually identical.

Two nonequivalent minima of exohedral BaC_{74} were found (Figure S4). Although the Ba−C distances are shorter by 8−11 pm, these configurations are less stable than the endohedral species by 235 and 208 kJ/mol, respectively.

The trajectory of the Ba atom inside the C_{74}-cage, obtained from Car−Parrinello molecular dynamics[48] calculations, mainly shows a movement of the endohedral Ba atom at one of the 3-fold degenerate minima of the potential surface perpendicular to the σ_h-plane of the C_{74}-cage, which is very similar to the trajectory of the europium atom in Eu@C_{74}.[25] The colored curves in Figure 6 display, over a time range of ≈17 ps, the variation of the distances from the Ba atom to specific carbon atoms (C(9), C(53), C(54)), which are part of the central 6:6 bonds of the three pyracylene units emphasized in Figure 5. The black curve shows the shortest distance of Ba to any carbon atom at any time step. It corresponds to an average Ba−C distance of 278 pm.

(48) Car, R.; Parrinello, M. *Phys. Rev. Lett.* **1985**, *55*, 2471−2474.

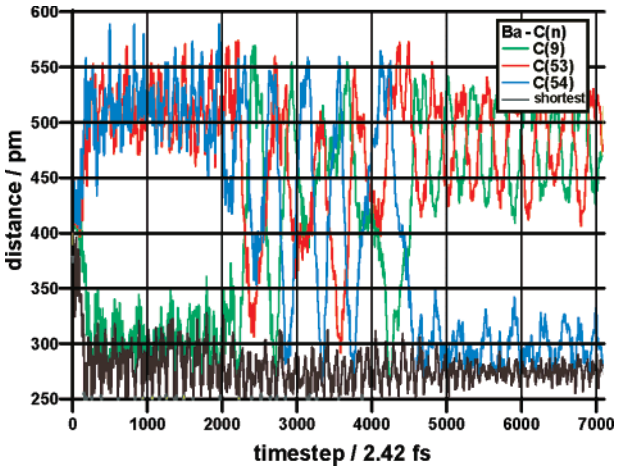

Figure 6. Results of Car−Parinello molecular dynamics simulations showing Ba−C distances to specific carbon atoms as well as the shortest distance of the barium atom to any carbon atom at any time step.

Discussion

Crystal structure determinations of fullerenes are seriously hampered by dynamic disorder of the nearly spherically shaped carbon cage molecules at higher temperatures and static disorder at low temperatures. The endohedral representatives, $M_n@C_{2m}$, encounter additional disorder due to rattling of the encaged metal. In employing diffraction techniques, computational chemistry, and XANES spectroscopy, in a synergetic manner, we have been able to determine the structure of endohedral Ba@C_{74} as a co-crystallizate with Co(OEP) and benzene. Different to earlier reports on monoatomic endohedral fullerenes, the encapsulated metal has been localized. Furthermore, only two orientations of the C_{74}-cage had to be assumed during the refinements.

The convergence of the least-squares fit of the diffraction data was significantly improved by using a rigid-body model for C_{74}^{2-} as determined by quantum chemical calculations. The local minimum structures calculated for Ba@C_{74} correspond to the 3-fold degenerate arrangements with barium located in one of the three pockets of the cloverleaf shaped molecule. In the crystal structure this degeneracy is lifted due to the intermolecular interactions between Co(OEP) and Ba@C_{74}. On contact with cobalt, the valence electrons on C_{74}^{2-} are being polarized, which, in turn, causes attraction of the barium cation.

The shortest Ba−C distances vary between 265 and 270 pm. For further comparison with other compounds, which contain Ba^{2+} cations and anionic carbon species, we note that the shortest Ba−C distances in exohedral fullerides Ba_6C_{60}[49] and Ba_3C_{60}[50] are 282.4 pm and 298.1 pm, respectively. In the various modifications of BaC_2,[51] the Ba−C distances vary in the range of 294.5 and 319.9 pm. The shortest Ba−C distances of the optimized structures of Ba@C_{74} obtained from the DFT calculations are between 278 and 289 pm.

As pointed out above, two split-positions and two orientations of the fullerene cage are observed. None of the four combinations of Ba-to-fullerene coordination (Figure 3) actually cor-

(49) Kortan, A. R.; Kopylov, N.; Glarum, S.; Gyorgy, E. M.; Ramirez, A. P.; Fleming, R. M.; Zhou, O.; Thiel, F. A.; Trevor, P. L.; Haddon, R. C. *Nature* **1992**, *360*, 566−568.
(50) Kortan, A. R.; Kopylov, N.; Fleming, R. M.; Zhou, O.; Thiel, F. A.; Haddon, R. C.; Rabe, K. M. *Phys. Rev. B* **1993**, *47*, 13070−13073.
(51) Vohn, V.; Kockelmann, W.; Ruschewitz, U. *J. Alloys Compd.* **1999**, *284*, 132−137.

respond to the coordination scheme deduced from the theoretical and XANES investigations. However, for Ba(1)−C_{74}(A) and Ba(2)−C_{74}(B) the closest Ba−C contacts are found in the vicinity of one or even two of such pyracylene units.

In this context, the question about the nature of the disorder phenomena arises. The two orientations of the pseudo-3-fold axis of the C_{74}-cage are rotated by an angle of about 92° against each other. Fullerene molecule A is orientated in such a way that one of the poles close to the pseudo-3-fold axis points toward the soup plate shaped Co(OEP) molecule. On the other hand, fullerene molecule B points with the vicinity of one of the three pyracylene units toward the Co(OEP). In either case the shortest C−Co contacts correspond to C atoms with a low angular sum (C(64A), C(34B), and C(38B)), which are located in the vicinity of a belt of atoms that exhibit high angular sums (Figure S3). Thus, both orientations of the fullerene cage correspond to configurations, which allow a large contact surface toward the π-system of the Co(OEP) molecule; i.e., these configurations seem to realize attractive $\pi-\pi$ and dispersion interactions, respectively. In the case of fullerene orientation B, one also finds one of the pyracylene units close to the Co(OEP) molecule. This may point toward a contribution of multipole−multipole interactions.

A detailed analysis is difficult, since the 2-fold negative charge of C_{74}^{2-} is mainly distributed over the whole cage and population analysis results should be interpreted very cautiously. However, there are some hints suggesting a slight accumulation of negative charge at the pyracylene units at the horizontal mirror plane of the C_{74} cage, which is increased by the coordinating Ba^{2+} cation. However, the Ba atom is highly mobile along the inner surface of the cage, a situation which can be deduced from structural investigations on other endohedral fullerenes, e.g., Ce@C_{82}.[52] Furthermore, the 2-fold positive charge of barium is incompletely shielded by the cage. Thus, a direct interaction between the cation and the Co(OEP) molecule has to be considered. Overall, the following types of interaction are in competition: (i) $\pi-\pi$ interaction, which forces the system toward an orientation with a low curvature at the fullerene to Co(OEP) interface; (ii) electrostatic interactions, which tend to orientate the highly curved regions of the fullerene (pyracylene units) toward the Co(OEP) molecule; and (iii) the direct interaction of the Ba^{2+} cation with the Co(OEP) molecule. As would be expected, the energy hypersurface exhibits more than one minimum, resulting in the orientational disorder present in the fullerene substructure.

Thus, the various coordination schemes of the endohedral metal atom found from quantum chemical and XANES investigations on one hand and from crystal structure analysis on the other hand are due to the intermolecular interactions present in the crystal structure of Ba@C_{74}·Co(OEP)·2C_6H_6.

The key problem with the X-ray absorption spectroscopic (XAS) part of this investigation is the lack of a reliable criterion for the position of the barium atom inside or outside of the C_{74}-cage. Virtually no suitable reference compounds are available which might allow a XANES fingerprint analysis. Furthermore, the local environments for the endo- and exohedral case, respectively, are not expected to be sufficiently characteristic for a successful EXAFS analysis. While a theoretical $\chi(k)$ obtained from a path development containing nearest-neighbor contributions does not point to a difference between those two configurations, the $\chi(k)$ function for all scattering paths exhibits pronounced differences in the low k-range (Figure S5). Thus, distinguishing between the different configurations using data from the multiple scattering region seems feasible. This expectation is fully confirmed in real-space full multiple scattering calculations which are suitable for the reproduction of the experimental XANES spectrum (Figure 4). Only the spectra calculated for the endohedral case show the characteristic double-peak structure at 5271 and 5279 eV, respectively. To check whether this double peak structure can serve as a valid indicator for a given structural environment, calculations with and without considering the core hole produced in the XAS measurements were performed. As expected for the calculation without a core hole, relaxation does not occur. As a consequence, the white line is consistently found at higher photon energies, for both the endo- and exohedral configurations, than experimentally measured.

The double maximum is not significantly influenced by an energy shift of 6 eV in the white line region. In comparison to the experimental value, the splitting between the white line and the double structure is underestimated in the simulations by about 3 eV. Two effects have to be considered to explain this behavior. On one hand, the amount of relaxation which occurs in the presence of a core hole is a function of valence-shell occupancy and is strongest for either a completely filled or a completely vacant orbital.[41] On the other hand, during the core-hole treatment realized in the FEFF8 code, the excited electron is placed into the lowest unoccupied state of the absorbing atom, which is then no longer unoccupied and thus shows a weaker trend toward relaxation. This effect can be circumvented by applying a $Z + 1$ model for the description of the core hole (Figure 4, right part). In fact, such a treatment leads to a significantly improved agreement between experiment and theory. However, the multiple-scattering fingerprint developed above is invariant under all of the described variations of the calculation parameters and thus can be considered to be a clear indicator for an endohedral configuration.

In addition, we have checked whether it is possible to exploit the information contained in the XANES spectra for an assessment of the precision of the quantum chemical geometry optimizations. For this purpose, the Ba L_{III} XANES spectra were calculated for varying positions of the Ba atom inside the fullerene. As can clearly be seen in Figure 7, a strong dependence of the shape resonances of the resulting spectra on the Ba positions assumed is observed with respect to both direction and distance of the central atom to the geometric center of the C_{74}-cage.

In fact, the configuration for which the experimentally measured position and shape of the white line and the characteristic twin-shape resonance have been observed corresponds to the Ba atom being shifted along path D (Figure 5) by 130 and 150 Å as shown in Figure 8. This confirms the results of the ab initio structure optimization and demonstrates the sensitivity of XANES for monitoring structural features of this cluster material.

The structural response of C_{74} upon 2-fold reduction is highly localized and manifests itself in a significant lengthening (Δd

(52) Rikiishi, Y.; Kubozono, Y.; Hosokawa, T.; Shibata, K.; Haruyama, Y.; Takabayashi, Y.; Fujiwara, A.; Kobayashi, S.; Mori, S.; Iwasa, Y. *J. Phys. Chem. B* **2004**, *108*, 7580−7585.

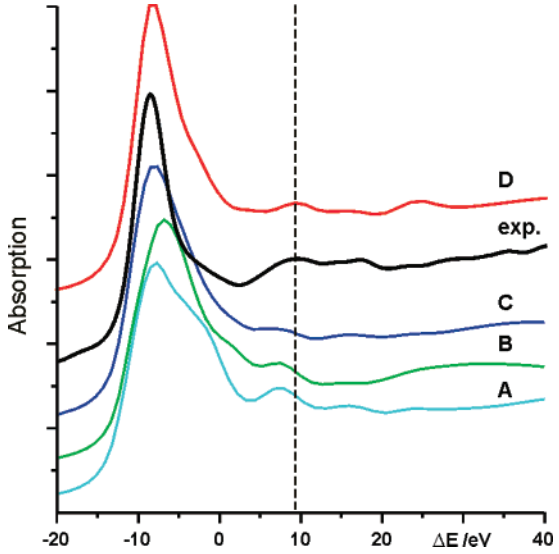

Figure 7. Calculated Ba L_{III} XANES spectra for a Ba atom inside a C_{74}-cage, shifted 150 pm off the geometric center of C_{74} (directions A−D as defined in Figure 5). The dashed line shows the position of the first maximum at 5271 eV of the double-peak found experimentally.

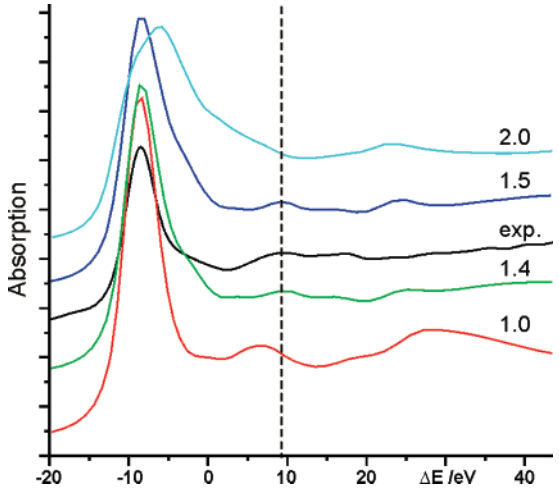

Figure 8. Calculated Ba L_{III} XANES spectra for Ba shifted along path D by 1.0, 1.3, 1.5, and 2 Å and the experimental spectrum.

= 2.8 pm) of the central 6:6 bonds of the pyracyclene units at the horizontal mirror plane and a shortening of the C−C bond in the vicinity of these 6:6 bonds. The coordination of the inner surface of the fulleride (C_{74}^{2-}) by a Ba atom leads on an average only to minor changes of the molecular structure of the carbon cage. Therefore, the molecular structure of C_{74}^{2-} is an adequate starting model for the rigid body refinement of the carbon cage of Ba@C_{74}.

The shortest Ba−C distance observed in the molecular dynamics simulations of Ba@C_{74} corresponds to an average value of 278 pm, irrespective of the carbon atom that is involved. It is remarkable that the Ba atom remains at this distance to the C_{74}-cage even when hopping from one of the three degenerate local minima to another, which occurs at temperatures above 500 K. This points to an effective inner surface at a constant distance to the C atoms of the cage. It should be noted, at this point, that the choice of the pseudopotential for the Ba atom is crucial, especially if a plane wave basis set is used. As an example, a detailed analysis is given for the BaC_2 molecule in the Supporting Information.

Conclusion

A variety of experimental and theoretical methods has been used in order to elucidate the structure of Ba@C_{74}. Microcrystal Synchrotron diffraction structure analysis of Ba@C_{74}·Co(OEP)·$2C_6H_6$ and XANES of a thin film sample of Ba@C_{74} individually and unambiguously prove the endohedral character of this monometallo fullerene. Experimental (XANES) and theoretical investigations point to a displacement by 130 to 150 pm of the endohedral atom from the center of gravity toward the central 6:6 bond of one of the three symmetry-equivalent pyracylene units at the horizontal mirror plane of the C_{74}-cage. Although molecular dynamics simulations of Ba@C_{74} exhibit jumps of the endohedral atom between the three symmetry-equivalent pyracylene units, the minimum Ba−C distance is virtually constant (278 pm). This points toward the motion of a hard sphere on top of an effective inner surface. The positional and orientational disorder of the Ba atom and the C_{74}-fullerene cage, as found in the crystal structure of Ba@C_{74}·Co(OEP)·$2C_6H_6$, is a consequence of the competition of $\pi-\pi$ and electrostatic interactions and the flat potential energy surface of the movement of the endohedral Ba atom along the inner surface. This results in two different C_{74}-to-Co(OEP) orientations and two different Ba positions.

Acknowledgment. The authors thank Martin Rieger for the assistance with the preparative work and Dr. Oliver Haufe for the separation of the fullerenes. Also we would like to thank Prof. Dr. Xianwen Wei for many good discussions and ideas.

Supporting Information Available: View on a (Ba@C_{74})-[Co(OEP)]$_2$(Ba@C_{74}) unit, MO schemes of C_{74}, C_{74}^{2-}, and Ba@C_{74}, structural response of C_{74} upon reduction and endohedral functionalization, figures of the different coordination geometries obtained from QCC, further XANES results, details about the structure, comparison of calculated structural data obtained with various methods, pseudopotenials, and basis sets. Quantum chemical calculations on the BaC_2 molecule to compare various methods, pseudopotentials and basis sets. X-ray crystallographic files in CIF format for Ba@C_{74}·Co(OEP)·$2C_6H_6$. Files for different local minima of the computed energy hypersurface containing the Cartesian coordinates of the atoms. This material is available free of charge via the Internet at http://pubs.acs.org.

JA0401693